

Research paper

Synthesis, cytotoxicity and structure-activity relationship of indolizinoquinolinedione derivatives as DNA topoisomerase IB catalytic inhibitors

Qian Yu ¹, Hui Yang ¹, Teng-Wei Zhu, Le-Mao Yu, Jian-Wen Chen, Lian-Quan Gu, Zhi-Shu Huang, Lin-Kun An ^{*}

School of Pharmaceutical Sciences, Sun Yat-sen University, Guangzhou, 510006, China

ARTICLE INFO

Article history:

Received 28 March 2018

Received in revised form

17 April 2018

Accepted 19 April 2018

Available online 22 April 2018

Keywords:

Indolizinoquinolinedione

Topoisomerase

Inhibitor

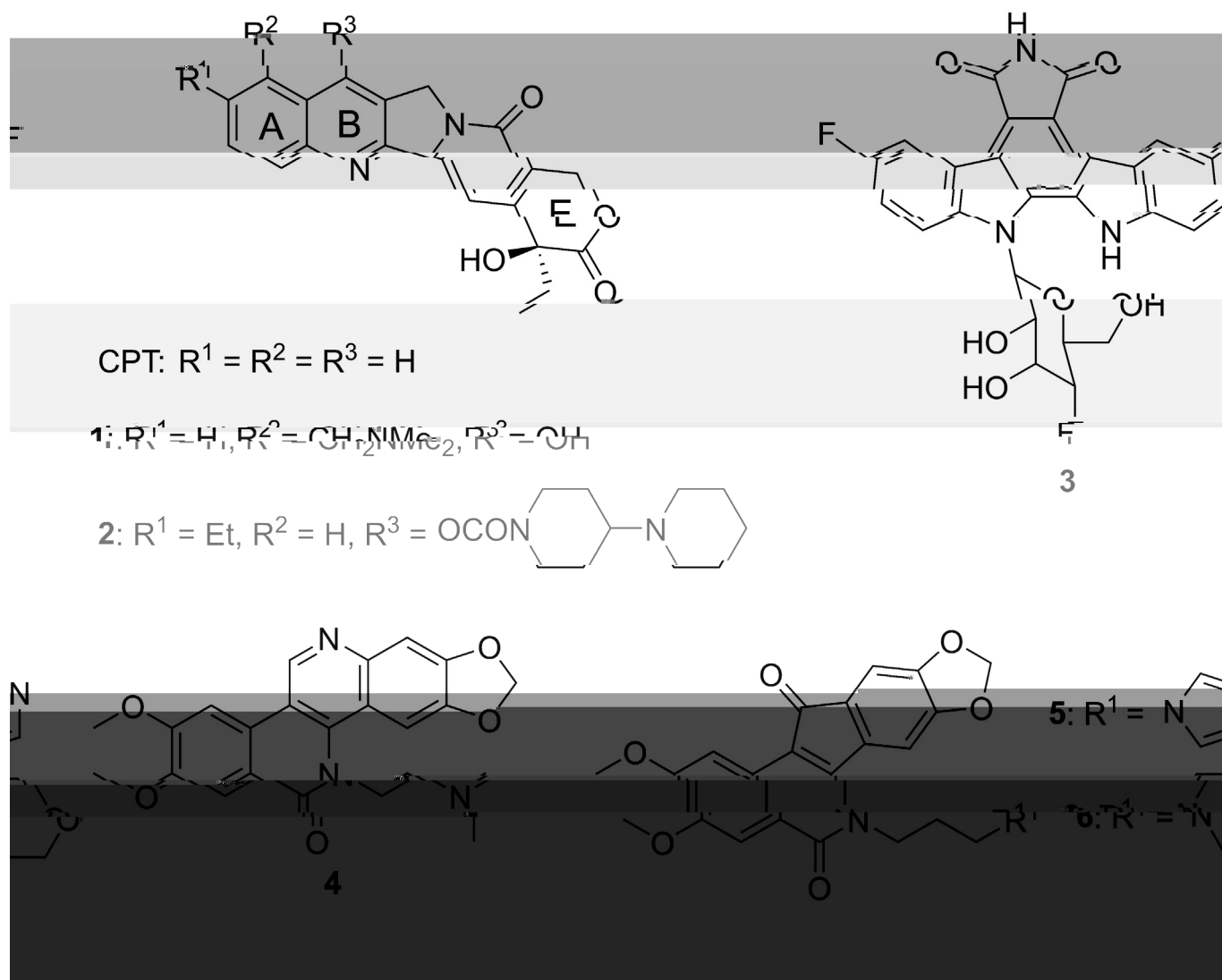
DNA damage

Cytotoxicity

ABSTRACT

Our previous studies reveal that indolizinoquinolinedione scaffold is a base to develop novel DNA topoisomerase IB (TOP1) catalytic inhibitors. In this work, twenty-three novel indolizinoquinolinedione derivatives were synthesized. TOP1-mediated relaxation, nicking and unwinding assays revealed that three fluorinated derivatives 26, 28 and 29, and one N,N-trans derivative 46 act as TOP1 catalytic inhibitors with higher TOP1 inhibition (++++), than camptothecin (++++) and without TOP1-mediated unwinding effect. MTT assay against five human cancer cell lines indicated that the highest cytotoxicity is 20 for CCRF-CEM cells, 25 for A549 and DU-145 cells, 26 for HCT116 cells, and 33 for Huh7 cells with GI_{50} values at nanomolar range. The drug-resistant cell assay indicated that compound

(A) Representative TOP1 poisons



(B) Our reported TOP1 catalytic inhibitors

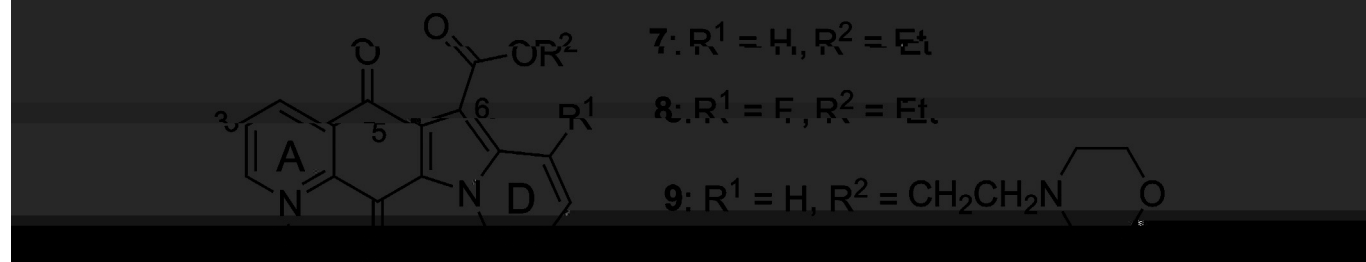


Fig. 1. Chemical structures of the representative TOP1 poisons (A) and our reported TOP1 catalytic inhibitors (B).

of a nitrogen atom in the A-ring is important for the cytotoxicity; 2) N,N-syn isomers have higher TOP1 inhibitory activity and cytotoxicity than the corresponding N,N-trans isomers; 3) the derivatives with electron-donating substituent at position 7 show poor cytotoxicity [20]. To investigate the effect of introduction of an electron-

withdrawing group at D-ring, and the position and number of nitrogen atom in the A-ring, three kinds of novel indolizinoquinolinedione derivatives were designed and synthesized based on the previous SAR. TOP1 inhibition and cytotoxicity were evaluated and reported here.

2. Results and discussion

2.1. Chemistry

According to the reported preparation [20,21], the indolizinoquinolinedione derivatives, for example 14 and 15 could be synthesized from the reaction of 6,7-dichloroquinoline-5,8-dione with ethyl acetoacetate and 3-halopyridine with low isolation yield in two steps (5% for 14 and 6% for 15 from 8-hydroxyl quinoline). In addition, the second step (cyclization reaction) gave four regioisomers [22], which were hard to isolate. To provide these compounds through an easier and effective method, a novel synthetic pathway was designed and explored. As shown in Scheme 1, the derivatives were prepared from the bromination of 8-hydroxyl

quinoline (10) [

22 and 23 were obtained by hydrolysis of compounds 13 and 14, respectively. Following acylchlorination of acids 22 and 23, esterification gave the target esters

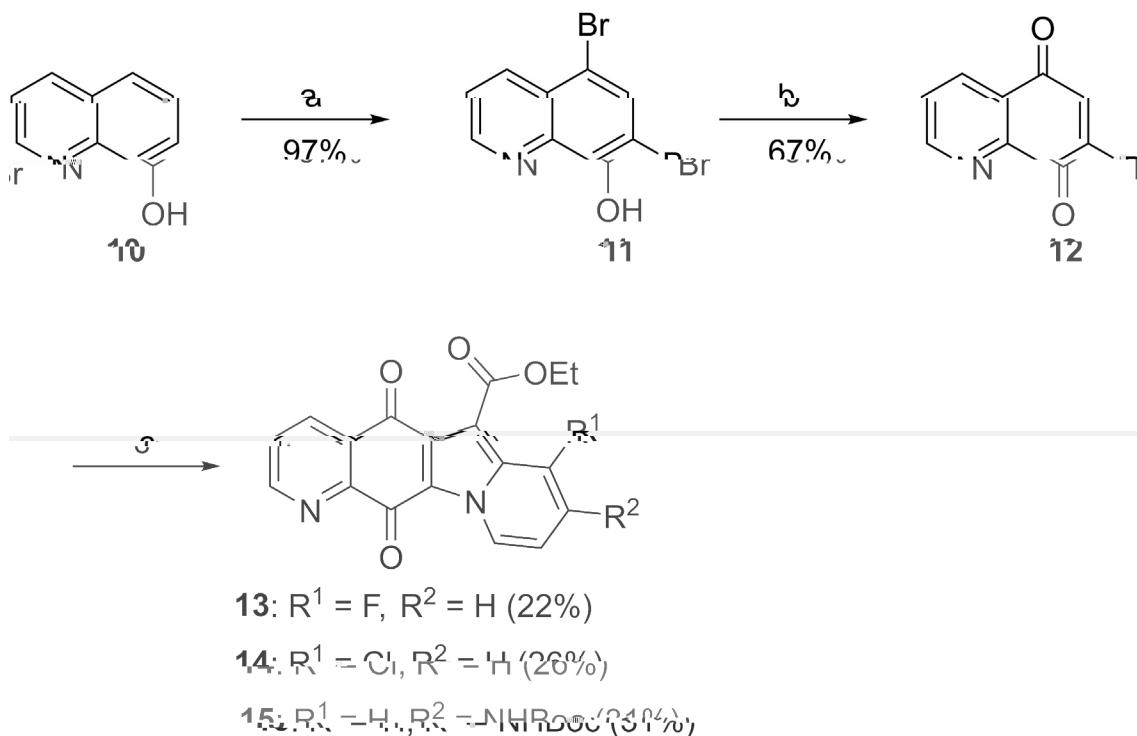
24–39.

To assess the effects of the position and number of nitrogen atom in the A-ring on the biological activity, compounds 46–48 were synthesized as shown in Scheme 4. Similar to the preparation of compounds 24–39, the products 46–48 were synthesized successively through hydrolysis, acyl chlorination and esterification reactions of materials 40–42 prepared in our laboratory [20,25,26].

The structures of all synthesized target compounds were characterized from ^1H and ^{13}C NMR, melting point, and HRMS data.

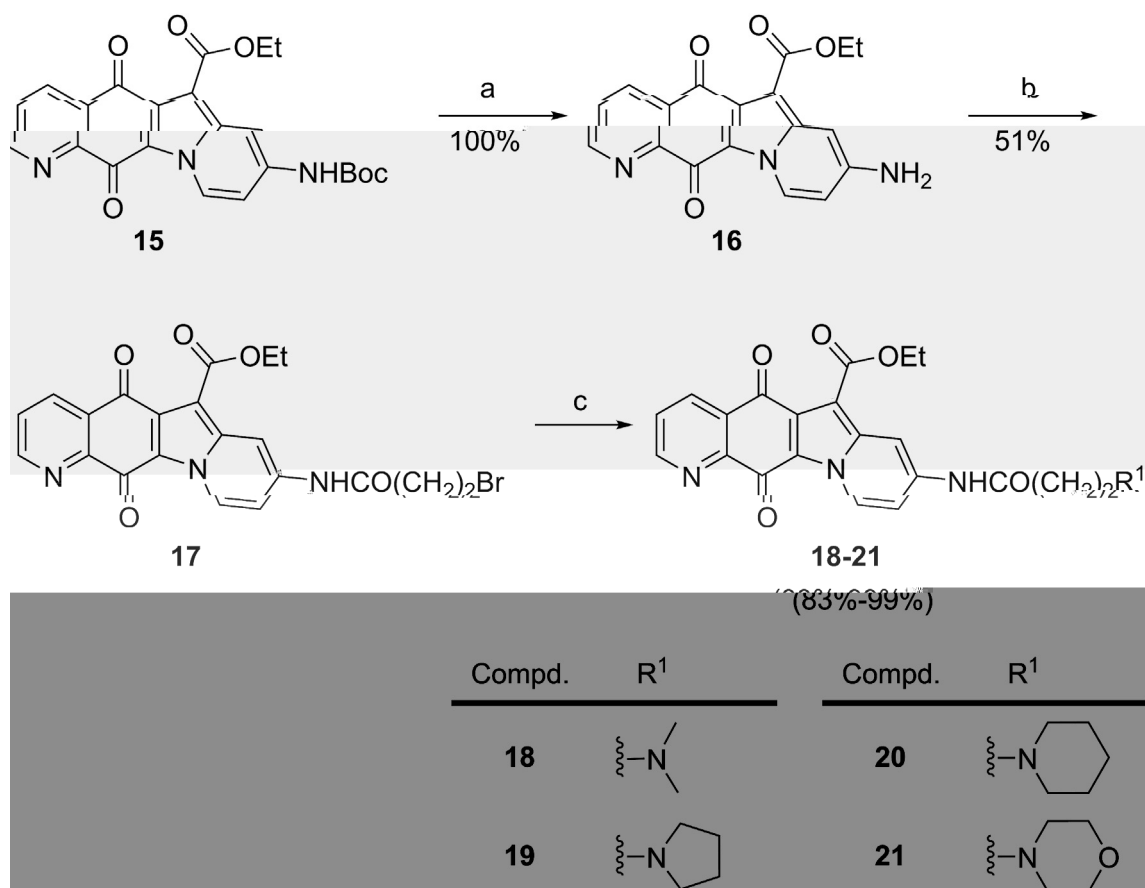
2.2. TOP1 inhibitory activities

TOP1 inhibitory activity of the target compounds was assessed by using TOP1-mediated relaxation assay with CPT as a positive control (Supplementary Information, Figs. S1 and S2), and semi-quantitatively expressed relative to CPT at 25 μM as follows: +, less than 40% of the activity; ++, between 41% and 80% of the activity; +++, between 81% and 120% of the activity; +++++, more than 121% of the activity. The TOP1 inhibitory activity is summarized in Table 1. Two 8-substituted derivatives 20 and 21 showed equipotent TOP1 inhibition to parent 7 (+++), while 18 and 19 had decreased TOP1 inhibition of ++, which indicated that the introduction of a weak electron-withdrawing group at position 8 is unable to improve the TOP1 inhibitory activity. Three fluorinated derivatives 26, 28 and 29, one chlorinated derivative 36 and one N,N-trans derivative 46 exhibited higher TOP1 inhibition than CPT and the parent 7. One fluorinated derivative 25 and one phthalazine derivative 48 exhibited equipotent inhibition (++++) to the parent 7. The N,N-trans derivative 46 with nitrogen atom at position 4 showed equipotent TOP1 inhibition to the corresponding derivative 9 (++++) with nitrogen atom at position 1 [13]. However, two nitrogen atoms in the A-ring, such as in compounds 47 (++) and 48 (+++), and the introduction of a halogen atom at position 7 (30 of + and 38 of ++) reduced TOP1 inhibition.



Scheme 1. The novel synthetic pathway of indolizinoquinolinedione derivatives.

Reagents and conditions: (a) Br_2 , NaHCO_3 , Na_2SO_3 , MeOH , rt. (b) *concd.* HNO_3 , *concd.* H_2SO_4 , $0\text{ }^\circ\text{C}$. (c) EtOH , pyridine derivatives, ethyl acetoacetate, reflux.



Scheme 2. Syntheses of compounds 18–21.

Reagents and conditions: (a) TFA, CH₂Cl₂, rt. (b) N₂, BrCH₂CH₂COCl, CHCl₃, Et₃N, rt. (c) amine materials (dimethylamine in Pressure Vessel), CHCl₃, K₂CO₃, KI, reflux.

Representative TOP1-mediated relaxation assay gels are shown in Fig. 2A. They show that compounds 26, 28 and 29 inhibit TOP1 activity in a dose-dependent manner. At high concentration (125 μM), these compounds showed stronger inhibitory activity than CPT with almost 100% of supercoiled DNA remaining, under condition where 58% supercoiled DNA remained for CPT. On the contrary, CPT showed higher inhibitory activity at low tested concentration (0.2 and 1 μM).

To explore the trapping TOP1cc ability of the synthesized compounds, compounds 26, 28 and 29 at 25 and 50 μM concentrations were tested in a TOP1-mediated nicking assay using excess TOP1. As shown in Fig. 2B, the TOP1 poison CPT could trap TOP1cc and increase the ratio of nicked DNA from 47% up to 49% at 50 μM concentration. On contrary, compounds 26, 28 and 29 significantly decreased the ratio of nicked DNA between 33% and 42%, imply they do not have ability to trap TOP1cc and act upstream of catalytic cleavage activity of TOP1 [11].

2.3. TOP1-mediated unwinding effect

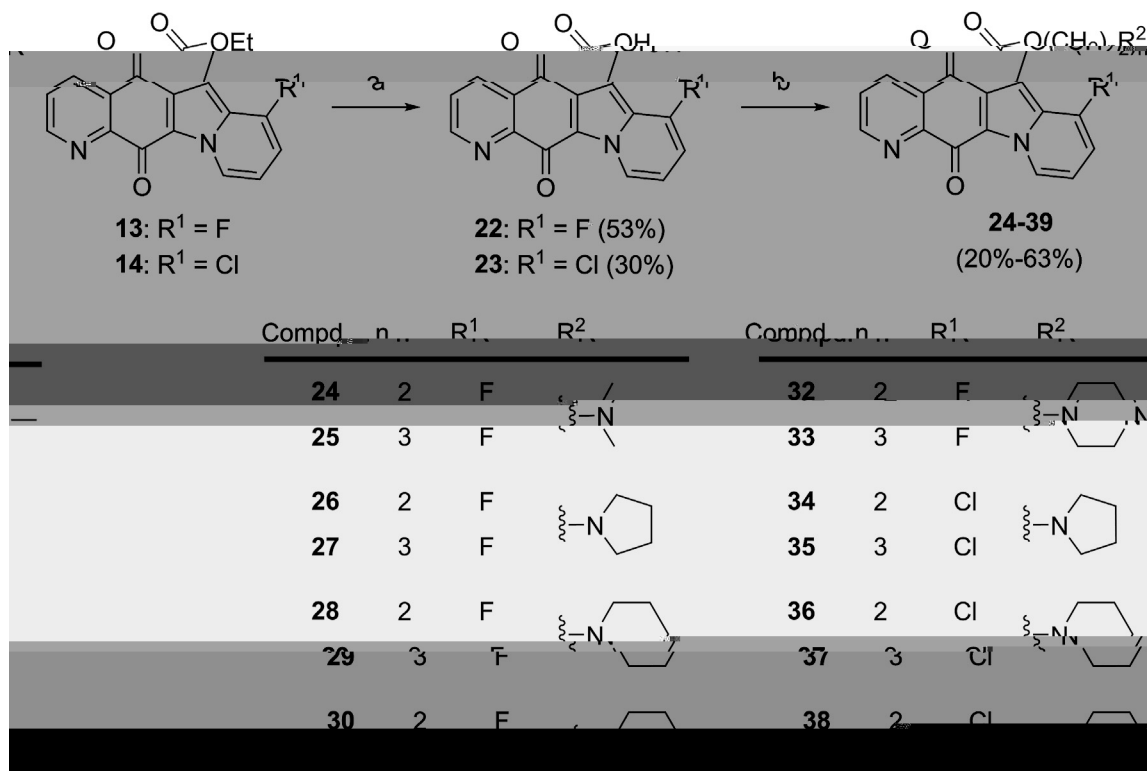
To assess whether the synthesized compounds induce DNA unwinding effect in the presence of excess TOP1, nine compounds (20, 21, 25, 26, 28, 29, 36, 46 and 48) with high TOP1 inhibition of +++ and ++++ were selected to be tested against TOP1-mediated unwinding assay using the DNA intercalator ethidium bromide (EB) as a positive control [27,28]. As shown in Fig. 2C (upper), EB exhibited clear unwinding effect with supercoiled pBR322 DNA as substrate. The representative compounds 26, 28 and 29 had no unwinding effect. In order to confirm these results,

TOP1-mediated unwinding assay with relaxed DNA as substrate was conducted [27]. As shown in Fig. 2C (bottom), compounds 26, 28 and 29 indeed had no unwinding effect. The results for all selected compounds are summarized in Table 1. Seven compounds 20, 21, 26, 28, 29, 46 and 48 have no unwinding effect up to 9 μM, implying that they inhibit TOP1 not through the mechanism of intercalating closed circular DNA [27,28], and are TOP1 catalytic inhibitors similar to the compounds 8 and 9 [11,13]. Among them, three fluorides 26, 28 and 29 exhibited high TOP1 inhibition of +++++, equal to their corresponding derivatives without fluorine atom, which showed obvious unwinding effect [13]. These results implied that fluorine atom at position 7 is worthy to be introduced for TOP1 inhibition. On the contrary, two selected compounds 25 and 36 showed obvious unwinding effects at 9 μM.

2.4. Cytotoxicities

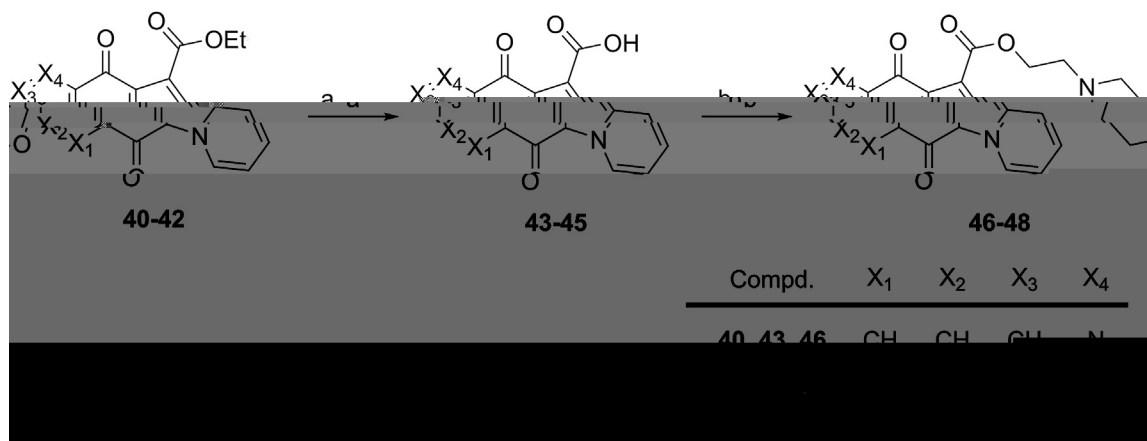
The cytotoxicity of the synthesized compounds was evaluated using MTT assay against five human tumor cell lines, including colon cancer (HCT116), leukemia (CCRF-CEM), non-small cell lung cancer (A549), hepatocarcinoma (Huh7) and prostate cancer (DU-145) cell lines. The compounds were incubated with cells for 72 h in a five-dose assay ranging from 10⁻⁸ to 10⁻⁴ M concentration. At the end of the incubation, MTT solution was added to test the percentage growth of tumor cells. The GI₅₀ values, defined as the concentration of the compound that resulted in 50% cell growth inhibition, were plotted and summarized in Table 1.

The compounds 18–21 with alkyl side chain at position 8 showed high cytotoxicity with GI₅₀ values at micromolar



Scheme 3. Syntheses of compounds 24–39.

Reagents and conditions: (a) 15% K₂CO₃, i-propanol, reflux, 24 h (b) i) SOCl₂, Et₃N, CHCl₃, reflux, 5 h; ii) alcohol materials, DMAP, CHCl₃, rt.



Scheme 4. Syntheses of compounds 46–48.

Reagents and conditions: (a) 15% K₂CO₃, i-propanol, reflux. (b) i) SOCl₂, Et₃N, CHCl₃, reflux, 5 h; ii) 2-morpholinoethanol, DMAP, CHCl₃, rt, 5 h.

concentration. And compound 20 showed the highest cytotoxicity against CCRF-CEM (GI₅₀ = 0.11 μM) with the equal TOP1 inhibition (++++) to parent 7.

Most of fluorine substituted derivatives 24–33 displayed potent cytotoxicity against five human tumor cells with GI₅₀ values at submicromolar or nanomolar levels. Compound 25 showed the highest cytotoxicity against A549 (GI₅₀ = 0.018 μM) and DU-145 (GI₅₀ = 0.025 μM) with equal TOP1 inhibition (++++) to parent 7. Compound 26 was the most potent against HCT116 cells with GI₅₀ of 0.023 μM and TOP1 inhibition of +++++. Although compound 33 had lower TOP1 inhibition (++) than parent 7, it showed the highest cytotoxicity against Huh7 cells (GI₅₀ = 0.042 μM). Although the chloride derivative 36 had equipotent TOP1 inhibition to its

corresponding fluoride derivative 28 (++++), it had decreased cytotoxicity for these five tumor cell lines, implying the presence of fluorine atom at position 7 is preferred. Comparing to the corresponding derivatives without halogen atom at position 7 [13], the fluorides 27–29 with pyrrolidinyl and piperidinyl terminus of side chain showed increased cytotoxicity against A549 cells, and the fluorides 30 and 31 with morpholinyl terminus and the chlorides 35–39 showed decreased cytotoxicity.

Although 46 (+++++) had higher and 48 (++++) had equipotent TOP1 inhibition with parent 7, they showed decreased cytotoxicity against these five human cancer cell lines, implying that the nitrogen atom at position 1 is important for cytotoxicity.

Table 1
TOP1 inhibitory activity, unwinding effect and cytotoxicity of the synthesized compounds.

Cpd.	Relaxation assay ^a	Unwinding effect	Cytotoxicity [GI ₅₀ ± SD (μM)] ^b				
			HCT116	CCRF-CEM	A549	Huh7	DU-145
7	+++	No	0.33 ± 0.009	0.68 ± 0.16	0.16 ± 0.089	0.85 ± 0.036	0.093 ± 0.001
18	++	– ^c	1.75 ± 0.18	0.29 ± 0.016	19.64 ± 5.36	1.65 ± 0.24	2.27 ± 0.21
19	++	–	1.90 ± 0.16	0.54 ± 0.054	29.26 ± 3.32	1.80 ± 0.24	0.70 ± 0.030
20	+++	No	1.43 ± 0.04	0.11 ± 0.010	2.65 ± 0.26	1.15 ± 0.22	3.12 ± 0.34
21	+++	No	0.30 ± 0.038	0.60 ± 0.073	9.68 ± 4.48	0.34 ± 0.07	16.43 ± 3.71
24	++	–	0.092 ± 0.041	1.09 ± 0.18	27.25 ± 0.23	0.31 ± 0.25	0.69 ± 0.12
25	+++	Yes	0.066 ± 0.050	0.37 ± 0.013	0.018 ± 0.002	0.080 ± 0.020	0.025 ± 0.008
26	++++	No	0.023 ± 0.015	0.79 ± 0.064	0.060 ± 0.15	0.12 ± 0.019	0.082 ± 0.025
27	++	–	0.029 ± 0.011	0.51 ± 0.042	0.080 ± 0.033	0.11 ± 0.045	0.092 ± 0.001
28	++++	No	0.025 ± 0.013	0.38 ± 0.10	0.29 ± 0.004	0.059 ± 0.050	0.091 ± 0.002
29	++++	No	0.027 ± 0.021	0.35 ± 0.021	0.072 ± 0.050	0.12 ± 0.016	0.21 ± 0.005
30	+	–	0.11 ± 0.013	1.10 ± 0.23	0.13 ± 0.017	0.57 ± 0.019	0.23 ± 0.026
31	+	–	0.038 ± 0.020	0.49 ± 0.078	0.23 ± 0.074	0.13 ± 0.072	0.25 ± 0.021
32	++	–	0.044 ± 0.030	0.45 ± 0.038	0.052 ± 0.012	0.11 ± 0.003	0.029 ± 0.006
33	++	–	0.044 ± 0.050	0.32 ± 0.021	0.021 ± 0.034	0.042 ± 0.012	0.073 ± 0.003
34	+	–	10.25 ± 1.11	48.23 ± 1.22	5.39 ± 0.30	2.25 ± 0.52	1.58 ± 0.23
35	+	–	38.25 ± 0.88	85.26 ± 8.31	24.46 ± 1.09	12.16 ± 0.95	8.32 ± 0.43
36	++++	Yes	0.31 ± 0.039	0.39 ± 0.013	0.12 ± 0.002	0.17 ± 0.10	2.52 ± 0.23
37	++	–	5.15 ± 0.50	5.35 ± 0.23	0.89 ± 0.022	1.32 ± 0.16	1.73 ± 0.081
38	++	–	28.56 ± 5.91	61.26 ± 5.09	48.59 ± 0.17	30.26 ± 0.15	29.49 ± 0.14
39	+	–	19.12 ± 0.56	68.56 ± 3.32	37.49 ± 0.38	28.45 ± 0.58	29.12 ± 0.26
46	++++	No	11.12 ± 0.38	70.52 ± 6.62	4.52 ± 2.42	14.15 ± 1.62	1.20 ± 0.052
47	++	–	13.15 ± 1.52	1.61 ± 0.22	8.52 ± 0.15	7.33 ± 1.10	2.55 ± 0.21
48	+++	No	3.43 ± 0.022	1.35 ± 0.17	0.86 ± 0.45	2.92 ± 0.34	1.22 ± 0.12
CPT	+++	–	0.009 ± 0.001	0.002 ± 0.001	0.003 ± 0.001	0.006 ± 0.001	0.019 ± 0.009

^a TOP1 inhibitory activity was semiquantitatively expressed relative to CPT at 25 μM as follows: +++++, more than 121% of the activity; +++, between 81% and 120% of the activity; ++, between 41% and 80% of the activity; +, less than 40% of the activity. Every experiment was repeated at least twice independently.

^b GI₅₀ values (means ± SD) were defined as the concentrations of compounds that resulted in 50% cell growth inhibition, and obtained from MTT assay. Every experiment was repeated at least three times.

^c “–” mean “not determined”.

2.5. Cytotoxicity of compound **26** in drug-resistant cell lines

To evaluate the cytotoxicity in drug-resistant cell lines, **26** was selected and tested by using MTT assay. The results were summarized in Table 2. HCT116-siTop1 subline was developed by transfection of colon cancer parental cells HCT116 with short hairpin RNA vectors expressing siRNA for TOP1 [29]. Comparing to the parental cell line HCT116, HCT116-siTop1 subline showed 8.3-fold resistant to CPT, of which TOP1 is the only known cellular target [7,15], and about 6.5-fold to indolizinoquinolinedione **26**, implying that TOP1 may be the major cellular target of **26**.

The prostate cancer cell RC0.1 has a R364H mutation in TOP1 relating to the wild-type parental cell DU-145 [30]. The TOP1 with R364H mutation is catalytically active, but lead to RC0.1 cells resistance to CPT because the R364 residue is close to the catalytic tyrosine and can stabilize the open form of TOP1cc [31,32]. The RC0.1 cells were highly resistant to TOP1 poison CPT (396.3-fold) and less resistant to compound **26** (36.8-fold), implying that the binding site of **26** on TOP1 is different from that of CPT.

P-glycoprotein (Pgp) mediated drug efflux is generally responsible for classical multiple drug resistance [33]. The chemotherapeutic agents doxorubicin (DOX) is substrate of Pgp, and has been found highly resistant for breast cancer MCF-7/ADR (77.8-fold) and hepatocellular HepG2/ADR sublines (47.6-fold), both with overexpressed Pgp [34]. However, compound **26** appeared to be less of Pgp substrates (Table 2).

2.6. Apoptosis analysis of compounds **26**, **28** and **29**

The effect of compounds **26**, **28** and **29** on apoptosis was estimated because they are TOP1 catalytic inhibitors with high TOP1 inhibition and cytotoxicity. Flow cytometry analysis using double staining with annexin V–FITC/PI was carried out in HCT116 cell line.

As shown in Fig. 3, after being treated with the tested compounds (1, 3, and 9 μM) for 12 h, the apoptotic cells increased obviously in a dose-dependent manner. Compounds **26**, **28** and **29** induced the major population of HCT116 cells into the late apoptotic stage (32.10%, 38.17% and 31.59%) at 9 μM concentration.

3. Conclusion

In summary, a series of indolizinoquinolinedione derivative were synthesized. TOP1-mediated assays revealed that the synthesized compounds act as TOP1 catalytic inhibitors and four compounds **26**, **28**, **29**, and **46** exhibit higher TOP1 inhibitory activity (+++++) than the parent **7** without TOP1-mediated unwinding effect up to 9 μM. The 8-substituted derivative **20** shows the highest cytotoxicity against CCRF-CEM cells with TOP1 inhibition of +++. The 7-fluorine substituted derivative **26** is the highest cytotoxicity against HCT116 cells with high TOP1 inhibition of +++++. Compound **33** shows the highest cytotoxicity against Huh7 cells with TOP1 inhibition of ++. Compound **25** shows the highest cytotoxicity against A549 and DU-145 with TOP1 inhibition of +++++. The drug-resistant cell assays indicated that **26** may mainly act to TOP1 in tumor cells and are less of Pgp substrates. Compounds **26**, **28** and **29** can effectively induce the apoptosis of HCT116 cells in a dose-dependent manner. This study indicates that the modification of indolizinoquinolinedione could provide novel TOP1 catalytic inhibitors with high cytotoxicity.

4. Methods and materials

4.1. General experiments

All starting materials and reagents for synthesis were commercially available and purchased from Sigma Aldrich Co,

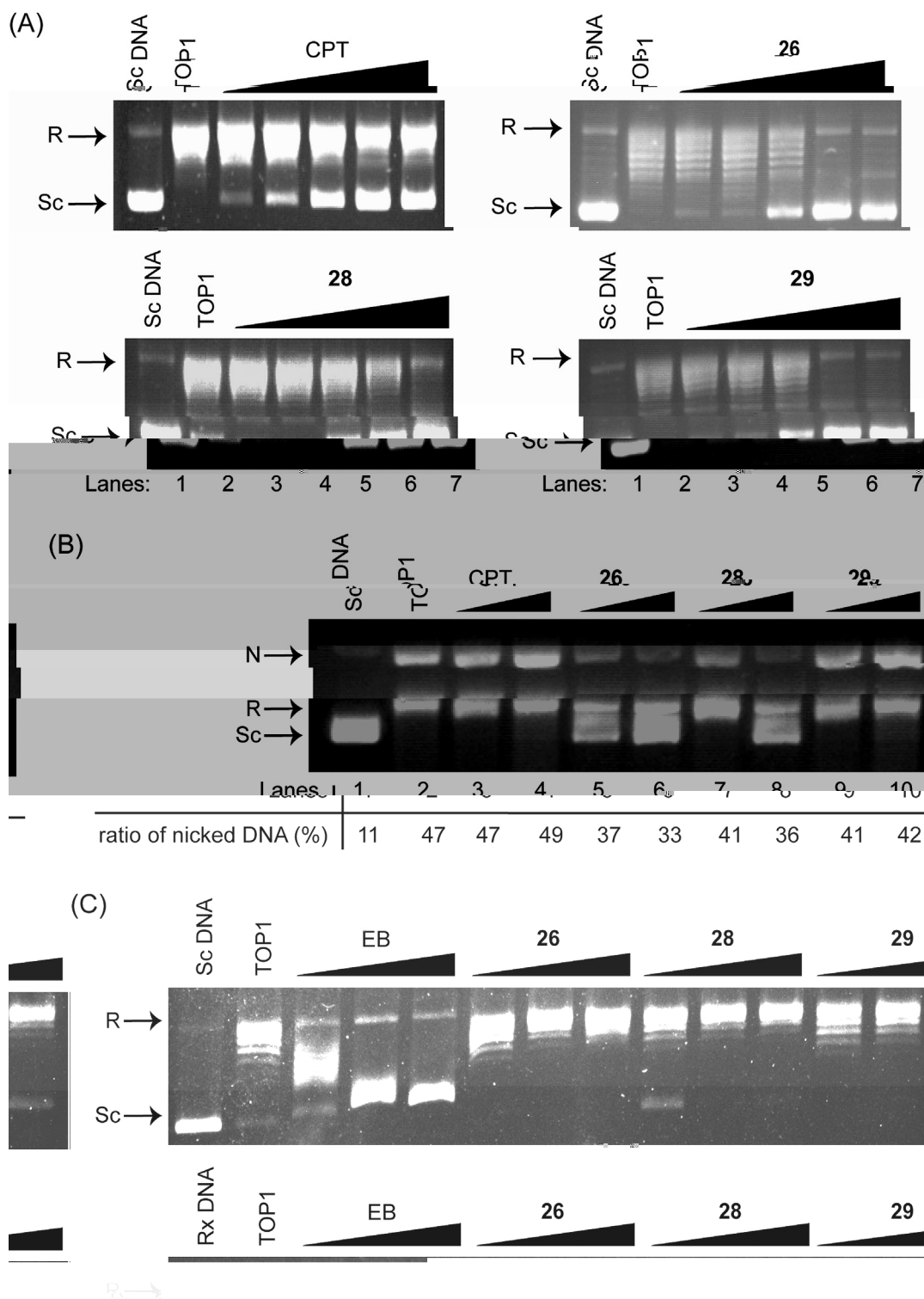


Fig. 2. (A) TOP1-mediated relaxation assay. Lane 1, supercoiled pBR322 DNA alone; Lane 2, DNA and TOP1; Lanes 3–7, DNA, TOP1 and tested compound at 0.2, 1, 5, 25, 125 μ M, respectively. (B) TOP1-mediated nicking assay. Lane 1, supercoiled pBR322 DNA alone; Lane 2, DNA and excess TOP1; Lanes 3–10, DNA, excess TOP1 and tested compound at 25, 50 μ M, respectively. (C) TOP1-mediated unwinding assay using supercoiled pBR322 DNA (upper) or relaxed pBR322 DNA (bottom) as substrate, respectively. Lane 1, DNA alone; Lane 2, DNA and excess of TOP1; Lanes 3–5, DNA, excess TOP1 and EB at 0.3, 0.6 and 1.2 mg/L; Lanes 6–14, DNA and excess TOP1 and tested compounds at 1, 3 and 9 μ M, respectively. R, relaxed DNA; Sc, supercoiled DNA; N, nicked DNA.

Table 2
Cytotoxicity of the compound **26** in drug-resistant human cancer cell lines.

Cpd.	GI ₅₀ ± SD (μM) ^a		Resistance Ratio ^b
	Parental cell line	Resistant subline	
26	HCT116	HCT116-siTop1	6.5
	0.023 ± 0.005	0.15 ± 0.029	
CPT	DU-145	RC0.1	8.3
	0.009 ± 0.001	0.075 ± 0.014	
26	MCF-7	MCF-7/ADR	36.8
	0.082 ± 0.025	2.94 ± 0.74	
CPT	HepG2	HepG2/ADR	396.3
	0.019 ± 0.009	7.53 ± 1.88	
26	MCF-7	MCF-7/ADR	1.1
	0.089 ± 0.15	0.097 ± 0.003	
DOX	HepG2	HepG2/ADR	77.8
	0.15 ± 0.003	11.67 ± 1.94	
26	MCF-7	MCF-7/ADR	7.5
	0.051 ± 0.027	0.38 ± 0.16	
DOX	0.19 ± 0.048	9.04 ± 0.14	47.6

^a GI₅₀ values (means ± SD) were defined as the concentrations of compounds that resulted in 50% cell growth inhibition and obtained from MTT assay. Every experiment was repeated at least three times.

^b Resistance ratio was

Aladdin Reagent Database Inc, and Alfa Aesar. High performance liquid chromatography (HPLC) was taken on a Shimadzu LC-10 A B. Mass spectra were analyzed on an Agilent 6120. HRMS were measured using an SHIMADZU LCMS-IT-TOF mass spectrometer. NMR spectra were performed on Bruker Avance III-400 spectrometer with TMS as an internal standard. Unless otherwise specified, chemical shifts (δ) were expressed in ppm with reference to the signals, and coupling constant (*J*) values were reported in Hz. Melting points were recorded on open capillary tubes on a MPA100 Optimelt Automated Melting Point System without being corrected. Silica gel (200–300 mesh, Qingdao Marine Chemical

Factory, Qingdao, China) was used for column chromatography. All compounds tested for biological activities were measured using HPLC and their purities were more than 95%.

Plasmid pBR322 DNA and calf thymus DNA TOP1 were purchased from Takara Biotechnology (Dalian). One unit of TOP1 was defined as the amount that relaxes 0.5 μg of pBR322 DNA at 37 °C for 30 min. The human wild-type cancer cell lines A549 and Huh7 were obtained from Laboratory Animal Center, Sun Yat-sen University. The human wild-type cancer cell lines HCT116, CCRF-CEM and DU-145, and the resistant cell lines HCT116-siTop1 and RC0.1 were a kind gift from Dr. Y. Pommier (Laboratory of Molecular Pharmacology, Center for Cancer Research, NCI, NIH). The human wild-type cancer cell lines MCF-7 and HepG2, and the resistant cell lines MCF-7/ADR and HepG2/ADR were a kind gift from Dr. X. Z. Bu (School of Pharmaceutical Sciences, Sun Yat-sen University).

4.2. Synthesis of compound **11**

Compound **11** was prepared according to the reported method [24]. The solution of bromine (3.1 mL, 60 mmol) in MeOH (30 mL) was added dropwise into the mixture 8-hydroxyquinoline (2.9 g, 20 mmol) and NaHCO₃ (3.36 g, 40 mmol) in MeOH (30 mL). After stirring for 5 min at room temperature, Na₂SO₃ (2.5 g, 20 mmol) and water (100 mL) were added and then the mixture was filtered and washed with water and dried in vacuo to give a white solid **11** (5.88 g, 97%). ¹H NMR (400 MHz, CDCl₃) δ 8.82 (dd, *J* = 4.2, 1.4 Hz, 1H), 8.46 (dd, *J* = 8.5, 1.5 Hz, 1H), 7.91 (s, 1H), 7.59 (dd, *J* = 8.5, 4.3 Hz, 1H). APCI-MS *m/z*: 301.9 (50%), 303.9 (100%), 305.9 (50%) [M+H]⁺.

4.3. Synthesis of compound **12**

The synthesis of compound **12** was carried out as the reported

method [23,24]. Concentrated HNO₃ (0.15 mL) was added dropwise to a solution of compound 11 (270 mg, 0.85 mmol) in concentrated H₂SO₄ (1 mL) in an ice bath. The reaction solution was stirred for 30 min and added with ice water (10 mL), and extracted with dichloromethane (5 mL x 3). The organic layer was concentrated under reduced pressure purified by silica gel column chromatography (dichloromethane/ethyl acetate: 30/1) to give a yellow solid (12, 136 mg), yield 67%. ¹H NMR (400 MHz, CDCl₃) δ 9.08 (dd, J = 4.7, 1.7 Hz, 1H), 8.44 (dd, J = 7.9, 1.7 Hz, 1H), 7.74 (dd, J = 7.9, 4.7 Hz, 1H), 7.62 (s, 1H). APCI-MS m/z: 237.9 (100%), 239.9 (100%) [M+H]⁺.

4.4. General procedure for synthesis of compounds 13–15

To a solution of 12 (1.0 g, 4.2 mmol) in EtOH (50 mL) was added dropwise into ethyl acetoacetate (1.64 g, 12.6 mmol). The reaction mixture was stirred at room temperature for 5 min. Pyridine derivatives (50 mmol) was added dropwise, and the reaction mixture was stirred at reflux for 16 h and extracted with dichloromethane (50 mL x 3). The organic layer was concentrated under reduced pressure purified by silica gel column chromatography (petroleum ether/ethyl acetate: 1/2) to give the target product.

Using 3-fluoropyridine or 3-chloropyridine as material, an orange red solid (22, 314 mg, 22%) or a red solid (23, 388 mg, 26%) was obtained, respectively. Their structures were characterized through ¹H and ¹³C NMR spectra, similar to our reported data [20].

4.4.1 Ethyl 8-((tert-butoxycarbonyl)amino)-5,12-dioxo-5,12-dihydroindolizino[2,3-g]quinoline-6-carboxylate (15)

Using the N-Boc protected 4-animopyridine as material, a red solid 15 (0.57 g) was obtained in 31% yield. ¹H NMR (400 MHz, CDCl₃) δ 9.76 (d, J = 7.2 Hz, 1H), 8.93 (dd, J = 4.8, 1.6 Hz, 1H), 8.46 (dd, J = 7.6, 1.6 Hz, 1H), 8.39 (d, J = 1.6 Hz, 1H), 7.55 (dd, J = 7.8, 4.6 Hz, 1H), 7.29 (d, J = 7.6 Hz, 1H), 6.83 (s, 1H), 4.44 (q, J = 7.1 Hz, 2H), 1.49 (s, 9H), 1.44 (t, J = 7.1 Hz, 3H). ¹³C NMR (100 MHz, CDCl₃) δ 179.2, 163.2, 153.9, 151.7, 149.6, 149.1, 141.6, 139.8, 135.3, 130.9, 129.4, 126.7, 122.6, 111.4, 105.4, 104.8, 100.0, 82.2, 61.1, 28.2, 14.3. The structure of 15 was also confirmed through 2D NMR spectrum. ESI-MS m/z: 436.1 [M+H]⁺.

4.5. Synthesis of compound 17

To the solution of compound 15 (435 mg, 1 mmol) in dichloromethane (20 mL), trifluoro acetic acid (4 mL) was added dropwise at room temperature. The reaction solution was stirred for 2 h and concentrated under reduced pressure. The red residue gel (crude compound 16) was dissolved in dried chloroform (20 mL). Under nitrogen, the solution was stirred and successively added Et₃N (1.4 mL) and a solution of pre-prepared 3-bromo propionyl chloride in chloroform (15 mL). The reaction solution was stirred for 8 h at room temperature and concentrated under reduced pressure. The residue was purified by silica gel column chromatography (dichloromethane/methanol: 50/1) to give an orange solid 17 (240 mg, 51%), which was used for the next preparation immediately. ESI-MS m/z: 470.1 (100%), 470.1 (100%) [M+H]⁺.

4.6. General procedure for the synthesis of compounds 18–21

The suspension of compound 17 (235 mg, 0.5 mmol), K₂CO₃ (134 mg, 1 mmol), KI (83 mg, 0.5 mmol), and amines (in Pressure Vessel for dimethylamine) in chloroform (50 mL) was stirred and heated under reflux overnight. The solvent was evaporated under reduced pressure. The residue was dissolved in TCM (50 mL). The organic layer was washed with water (10 mL x 2) and saturated aqueous saline (10 mL), and dried with anhydrous MgSO₄. The

solvent was evaporated under reduced pressure. The resulting residue was purified by using silica gel column chromatography to give the target product.

4.6.1. Ethyl-8-(3-(dimethylamino)propanamido)-5,12-dioxo-5,12-dihydroindolizino[2,3-g]quinoline-6-carboxylate (18)

Using the mixture of dichloromethane and methanol (10:1) as eluent to give orange powder, yield 88%, mp = 250.9–251.5 °C. ¹H NMR (400 MHz, CD₃OD) δ 11.74 (s, 1H), 9.76 (d, J = 7.5 Hz, 1H), 8.92 (d, J = 4.6, 1.6 Hz, 1H), 8.49 (s, 1H), 8.46 (d, J = 7.9 Hz, 1H), 7.54 (dd, J = 7.9, 4.7 Hz, 1H), 7.37 (d, J = 7.5 Hz, 1H), 4.44 (q, J = 7.1 Hz, 2H), 2.64 (t, J = 6.0 Hz, 2H), 2.50 (t, J = 6.0 Hz, 2H), 2.37 (s, 6H), 1.46 (t, J = 7.5 Hz, 3H). ¹³C NMR (100 MHz, CD₃OD) δ 178.8, 171.7, 171.3, 162.4, 153.7, 149.1, 140.4, 139.5, 134.5, 130.3, 128.8, 127.9, 127.8, 122.5, 112.1, 105.1, 103.5, 60.2, 54.7, 44.4, 34.5, 14.1. HRMS (ESI) m/z: 435.1653 [M+H]⁺, calcd for C₂₃H₂₃N₄O₅ 435.1668.

4.6.2. Ethyl 5,12-dioxo-8-(3-(pyrrolidin-1-yl)propanamido)-5,12-dihydroindolizino[2,3-g]quinoline-6-carboxylate (19)

Using the mixture of dichloromethane and methanol (10:1) as eluent to give orange powder, yield 85%, mp = 265.5–266.8 °C. ¹H NMR (400 MHz, CD₃OD) δ 10.95 (s, 1H), 9.69 (d, J = 7.3 Hz, 1H), 9.00 (s, 1H), 8.80 (s, 1H), 8.43 (d, J = 8.0 Hz, 1H), 7.81 (dd, J = 7.5, 4.7 Hz, 1H), 7.48 (d, J = 7.5 Hz, 1H), 4.33 (q, J = 7.0 Hz, 2H), 3.47 (t, J = 7.0 Hz, 2H), 3.10 (t, J = 7.0 Hz, 2H), 2.95 (t, J = 7.0 Hz, 4H), 1.41 (t, J = 7.0 Hz, 4H), 1.23 (s, 3H). ¹³C NMR (100 MHz, CD₃OD) δ 179.6, 172.4, 169.6, 163.0, 154.2, 149.5, 140.8, 139.7, 135.2, 130.9, 128.5, 127.8, 127.3, 123.1, 112.6, 105.8, 104.0, 60.8, 53.8, 53.8, 49.7, 32.8, 22.8, 22.8, 14.3. HRMS (ESI) m/z: 461.1823 [M+H]⁺, calcd for C₂₅H₂₅N₄O₅ 461.1825.

4.6.3. Ethyl 5,12-dioxo-8-(3-(piperidin-1-yl)propanamido)-5,12-dihydroindolizino[2,3-g]quinoline-6-carboxylate (20)

Using the mixture of dichloromethane and methanol (10:1) as eluent to give purple powder, yield 99%, mp = 259.3–261.2 °C. ¹H NMR (400 MHz, CD₃OD) δ 12.08 (s, 1H), 9.82 (d, J = 7.2 Hz, 1H), 8.99 (d, J = 3.7 Hz, 1H), 8.70 (s, 1H), 8.53 (d, J = 7.5 Hz, 1H), 7.74–7.56 (m, 1H), 7.40 (d, J = 6.6 Hz, 1H), 4.50 (dd, J = 13.8, 6.8 Hz, 2H), 2.72–2.80 (m, 6H), 1.77–1.84 (m, 4H), 1.60–1.68 (m, 2H), 1.51 (t, J = 7.0 Hz, 2H), 1.26 (t, J = 7.1 Hz, 3H). ¹³C NMR (100 MHz, CD₃OD) δ 179.3, 172.3, 170.5, 163.0, 154.2, 149.7, 140.9, 139.9, 135.1, 130.9, 129.5, 128.4, 127.7, 123.0, 112.6, 105.7, 104.0, 60.7, 53.4, 53.4, 52.6, 34.5, 24.2, 24.2, 22.8, 14.1. HRMS (ESI) m/z: 475.1967 [M+H]⁺, calcd for C₂₆H₂₇N₄O₅ 475.1981.

4.6.4. Ethyl 8-(3-morpholinopropanamido)-5,12-dioxo-5,12-dihydroindolizino[2,3-g]quinoline-6-carboxylate (21)

Using the mixture of dichloromethane and methanol (10:1) as eluent to give orange powder, yield 83%, mp = 267.9–269.7 °C. ¹H NMR (400 MHz, CD₃OD) δ 11.60 (s, 1H), 9.84 (d, J = 7.5 Hz, 1H), 8.99 (d, J = 3.0 Hz, 1H), 8.62 (s, 1H), 8.49 (d, J = 7.5 Hz, 1H), 7.62 (dd, J = 7.5, 4.7 Hz, 1H), 7.45 (d, J = 6.0 Hz, 1H), 4.51 (q, J = 7.0 Hz, 2H), 3.89 (s, 4H), 2.80 (d, J = 5.5 Hz, 2H), 2.70 (s, 4H), 2.63 (d, J = 5.7 Hz, 2H), 1.52 (t, J = 7.1 Hz, 3H). ¹³C NMR (100 MHz, CD₃OD) δ 178.8, 171.8, 171.5, 162.4, 153.8, 149.0, 140.4, 139.4, 134.4, 130.2, 128.8, 127.9, 127.1, 122.4, 112.1, 105.0, 103.3, 66.1, 60.1, 53.7, 52.9, 34.1, 14.1. HRMS (ESI) m/z: 477.1756 [M+H]⁺, calcd for C₂₅H₂₅N₄O₆ 477.1774.

4.7. Hydrolysis of compounds 13 and 14

The ester analogues 13 or 14 (1 mmol) were hydrolyzed with K₂CO₃ (15%) in isopropanol solution (100 mL) to give the acid analogues 22 or 23, respectively.

4.7.1. 7-Fluoro-5,12-dioxo-5,12-dihydroindolizino[2,3-g]quinoline-6-carboxylic acid (**22**)

Amaranth solid, yield 53%, mp = 281–282

437.1622 [M+H]⁺, calcd for C₂₃H₂₂FN₄O₄ 437.1620.

4.8.10. 3-(4-Methylpiperazin-1-yl)propyl-7-fluoro-5,12-dioxo-5,12-dihydroindolizino[2,3-g]quinoline-6-carboxylate (**33**)

Using the mixture of dichloromethane and methanol (10:1) as eluent to give red powder, yield 38%, mp = 127.2–128.1 °C. ¹H NMR (400 MHz, CDCl₃) δ 9.65 (d, J =

using TOP1-mediated relaxation assay [35]. Briefly, reaction mixture (20 μ L) with 0.5 μ g supercoiled pBR322 DNA in Relaxation Buffer (10 mM Tris-HCl, pH 7.5, 50 mM KCl, 5 mM MgCl₂, 15 μ g/mL BSA, 40 μ g/mL DTT) was incubated with 1 unit of calf thymus TOP1 in the absence or in the presence of compound for 30 min at 37 °C. Then the reaction solution was added with 6 \times loading buffer (4 μ L), and was analyzed using a 0.8% agarose gel in TBE buffer at 4.6 V/cm for 1.5 h. Gel was stained with 1 \times gel red for 30 min and subsequently visualized with a UV transilluminator.

4.10. TOP1-mediated nicking assay

The nicking reaction (40 μ L) containing 30 units of TOP1 and the tested compound was initiated by the addition of 0.5 μ g supercoiled pBR322 DNA in Reaction Buffer and allowed to be incubated for 30 min at 37 °C. The reaction was terminated by addition of SDS (final concentration of 1%) [15]. After digestion with proteinase K (final concentration of 1 mg/mL) for 30 min at 55 °C, samples were mixed with 4 μ L loading buffer and analyzed in a 1% agarose gel in TAE buffer at 3 V/cm for 30 min. Then the gel was put in the TAE buffer containing 0.125 μ g/mL of EB for 30 min. Finally, the gel was run in TAE buffer for another 30 min and visualized with a UV transilluminator.

4.11. TOP1-mediated unwinding

TOP1-mediated cleavage assay was carried out as described with slight modification [27]. Briefly, the reaction solution (20 μ L) with 0.2 μ g supercoiled pBR322 DNA or relaxed pBR322 DNA as substrate and 20 units of TOP1 was performed in Relaxation Buffer. The compound was incubated with DNA at room temperature for 10 min prior to the addition of excess TOP1. And then, the reaction solution was incubated for 30 min at 37 °C. The reaction was terminated by addition of 5 μ L solution containing 5% of SDS and 5 mg/mL proteinase K. The DNA intercalator Ethidium bromide was used as a positive control. The sample was added with 5 μ L 6 \times loading buffer, and was analyzed using a 0.8% agarose gel in TBE buffer at 4.6 V/cm for 1.5 h. Gel was stained with 1 \times gel red for 30 min and visualized with a UV transilluminator.

4.12. Cell culture and MTT assay

The cells were cultured on RPMI-1640 or DMEM medium at 37 °C in a humidified atmosphere with 5% CO₂. All cells to be tested in the following assays had a passage number of 3–6.

For the drug treatment experiments, the cancer cells were treated with the compounds (predissolved in DMSO) at a five-dose assay ranging from 10⁻⁸ to 10⁻⁴ M concentration. After incubation for 72 h at 37 °C, MTT solution (50 μ L, 1 mg/mL) in PBS (PBS without MTT as the blank) was fed to each well of the culture plate (containing 100 μ L medium). After 4 h incubation, the formazan crystal formed in the well was dissolved with 100 μ L of DMSO for optical density reading at 570 nm [36]. The GI₅₀ value was calculated by nonlinear regression analysis (GraphPad Prism).

4.13. Flow cytometry

HCT116 cells (3.0 \times 10⁵ cells/mL) were grown in culture medium on 6-well plates treated with various concentrations of compound or untreated for 12 h. And then, the cells were harvested and washed with cold PBS buffer, resuspended in 1 \times binding buffer, and then stained with 5 μ L FITC Annexin V and 5 μ L propidium iodide (KeyGen BioTech, China) for 15 min in dark. The stained cells were analyzed by using flow cytometry (BD, FACSCalibur, USA) within 1 h. The experiments were repeated independently for three times.

Acknowledgements

This work is supported by the National Natural Science Foundation of China (No. 81373257 and 81703668), Guangdong Natural Science Fund (No. S2013010015609 and 2017A030310396).

Appendix A. Supplementary data

Supplementary data related to this article can be found at <https://doi.org/10.1016/j.ejmech.2018.04.040>.

References

- [1] J.J. Champoux, DNA topoisomerases: structure, function, and mechanism, *Annu. Rev. Biochem.* 70 (2001) 369–413.
- [2] L. Stewart, M.R. Redinbo, X. Qui, W.G.J. Hol, J.J. Champoux, A model for the mechanism of human topoisomerase I, *Science* 279 (1998) 1534–1541.
- [3] J.M. Berger, S.J. Gamblin, S.C. Harrison, J.C. Wang, Structure and mechanism of DNA topoisomerase II, *Nature* 379 (1996) 225–232.
- [4] Y. Pommier, Y. Sun, S.N. Huang, J.L. Nitiss, Roles of eukaryotic topoisomerases in transcription, replication and genomic stability, *Nat. Rev. Mol. Cell Biol.* 17 (2016) 703–721.
- [5] B. Szczesny, A. Brunyanski, A. Ahmad, G. Olah, C. Porter, T. Toliver-Kinsky, L. Sidosis, D.N. Herndon, C. Szabo, Time-dependent and organ-specific changes in mitochondrial function, mitochondrial DNA integrity, oxidative stress and mononuclear cell infiltration in a mouse model of burn injury, *PLoS One* 10 (2015), e0143730.
- [6] Y. Pommier, Drugging topoisomerases: lessons and challenges, *ACS Chem. Biol.* 8 (2013) 82–95.
- [7] Y. Pommier, Topoisomerase I inhibitors: camptothecins and beyond, *Nat. Rev. Canc.* 6 (2006) 789–802.
- [8] Y. Pommier, DNA topoisomerase I inhibitors: chemistry, biology, and interfacial inhibition, *Chem. Rev.* 109 (2009) 2894–2902.
- [9] Y. Pommier, E. Leo, H. Zhang, C. Marchand, DNA topoisomerases and their poisoning by anticancer and antibacterial drugs, *Chem. Biol.* 17 (2010) 421–433.
- [10] M.E. Ashour, R. Atteya, S.F. El-Khamisy, Topoisomerase-mediated chromosomal break repair: an emerging player in many games, *Nat. Rev. Canc.* 15 (2015) 137–151.
- [11] N. Wu, X.W. Wu, K. Agama, Y. Pommier, J. Du, D. Li, L.Q. Gu, Z.S. Huang, L.K. An, A novel DNA topoisomerase I inhibitor with different mechanism from camptothecin induces G2/M phase cell cycle arrest to K562 cells, *Biochemistry* 49 (2010) 10131–10136.
- [12] A. Ganguly, B. Das, A. Roy, N. Sen, S.B. Dasgupta, S. Mukhopadhyay, H.K. Majumder, Betulinic acid, a catalytic inhibitor of topoisomerase I, inhibits reactive oxygen species-mediated apoptotic topoisomerase I-DNA cleavable complex formation in prostate cancer cells but Chiraphorbolol inhibits the complex formation, *PLoS One* 14 (2019) e0200000.

- [22] X.W. Wu, Z.P. Wu, L.X. Wang, H.B. Zhang, J.W. Chen, W. Zhang, L.Q. Gu, Z.S. Huang, L.K. An, Synthesis, antimicrobial activity and possible mechanism of action of 9-bromo-substituted indolizinoquinoline-5,12-dione derivatives, *Eur. J. Med. Chem.* 46 (2011) 4625–4633.
- [23] H.Y. Choi, D.Y. Chi, Simple preparation of 7-alkylamino-2-methylquinoline-5,8-diones: regiochemistry in nucleophilic substitution reactions of the 6- or 7-bromo-2-methylquinoline-5,8-dione with amines, *Tetrahedron* 60 (2004) 4945–4951.
- [24] H. Hussain, S. Specht, S.R. Sarite, A. Hoerauf, K. Krohn, New quinoline-5,8-dione and hydroxynaphthoquinone derivatives inhibit a chloroquine resistant *Plasmodium falciparum* strain, *Eur. J. Med. Chem.* 54 (2012) 936–942.
- [25] D.Q. Shen, Z.P. Wu, X.W. Wu, Z.Y. An, X.Z. Bu, L.Q. Gu, Z.S. Huang, L.K. An, Synthesis and antiproliferative activity of indolizinothalazine-5,12-dione derivatives, DNA topoisomerase IB inhibitors, *Eur. J. Med. Chem.* 45 (2010) 3938–3942.
- [26] D.Q. Shen, N. Wu, Y.P. Li, Z.P. Wu, H.B. Zhang, Z.S. Huang, L.Q. Gu, L.K. An, Design, synthesis, and cytotoxicity of indolizinoquinoline-5,12-dione derivatives, novel DNA topoisomerase IB inhibitors, *Aust. J. Chem.* 63 (2010) 1116–1121.
- [27] Y. Pommier, J.M. Covey, D. Kerrigan, J. Markovits, R. Pham, DNA unwinding and inhibition of mouse leukemia L1210 DNA topoisomerase I by intercalators, *Nucleic Acids Res.* 15 (1987) 6713–6731.
- [28] H.M. Berman, P.R. Young, The interaction of intercalating drugs with nucleic acids, *Annu. Rev. Biophys. Bioeng.* 10 (1981) 87–114.
- [29] Z.H. Miao, A. Player, U. Shankavaram, Y.H. Wang, D.B. Zimonjic, P.L. Lorenzi, Z.Y. Liao, H. Liu, T. Shimura, H.L. Zhang, L.H. Meng, Y.W. Zhang, E.S. Kawasaki, N.C. Popescu, M.I. Aladjem, D.J. Goldstein, J.N. Weinstein, Y. Pommier, Nonclassic functions of human topoisomerase I: genome-wide and pharmacologic analyses, *Canc. Res.* 67 (2007) 8752–8761.
- [30] Y. Urasaki, G.S. Laco, P. Pourquier, Y. Takebayashi, G. Kohlhaagen, C. Gioffre, H. Zhang, D. Chatterjee, P. Pantazis, Y. Pommier, Characterization of a novel topoisomerase I mutation from a camptothecin resistant human prostate cancer cell line, *Canc. Res.* 61 (2001) 1964–1969.
- [31] B.L. Staker, K. Hjerrild, M.D. Feese, C.A. Behnke, A.B. Burgin Jr., L. Stewart, The mechanism of topoisomerase I poisoning by a camptothecin analog, *Proc. Natl. Acad. Sci. U.S.A.* 99 (2002) 15387–15392.
- [32] B.L. Staker, M.D. Feese, M. Cushman, Y. Pommier, D. Zembower, L. Stewart, A.B. Burgin, Structures of three classes of anticancer agents bound to the human topoisomerase I-DNA covalent complex, *J. Med. Chem.* 48 (2005) 2336–2345.
- [33] C.P. Wu, C.H. Hsieh, Y.S. Wu, The emergence of drug transporter-mediated multidrug resistance to cancer chemotherapy, *Mol. Pharm.* 8 (2011) 1996–2011.
- [34] J. Zhu, R. Wang, L. Lou, W. Li, G. Tang, X. Bu, S. Yin, Jatrophone diterpenoids as modulators of P-Glycoprotein-Dependent multidrug resistance (MDR): advances of structure-activity relationships and discovery of promising MDR reversal agents, *J. Med. Chem.* 59 (2016) 6353–6369.
- [35] L.F. Liu, K.G. Miller, Eukaryotic DNA topoisomerases: two forms of type I DNA topoisomerases from HeLa cell nuclei, *Proc. Natl. Acad. Sci. U.S.A.* 78 (1981) 3487–3491.
- [36] J. Carmichael, W.G. DeGraff, A.F. Gazdar, J.D. Minna, J.B. Mitchell, Evaluation of a tetrazolium-based semiautomated colorimetric assay: assessment of chemosensitivity testing, *Canc. Res.* 47 (1987) 936–942.